Nitrilotriacetic Amine-Functionalized Polymeric Core-Shell Nanoparticles as Enzyme Immobilization Supports

Dominic Keller,[a,b] *Ana Beloqui,*[a,b,‡] *Mónica Martínez-Martínez,*[c] *Manuel Ferrer,*[c] *Guillaume Delaittre*[a,b,]*

[a]Institute of Toxicology and Genetics, Karlsruhe Institute of Technology (KIT), Hermann-von-Helmholtz-Platz 1, 76344 Eggenstein-Leopoldshafen, Germany
[b]Preparative Macromolecular Chemistry, Institute for Technical Chemistry and Polymer Chemistry, Karlsruhe Institute of Technology (KIT), Engesserstrasse 15, 76131 Karlsruhe, Germany
[c]Institute of Catalysis, Consejo Superior de Investigaciones Científicas, Marie Curie 2, 28049 Madrid, Spain
[‡]Present Address: Nanomaterials group, CICnanoGUNE, Avenida Tolosa 76, 20018 Donostia-San Sebastián, Spain

ABSTRACT Nitrilotriacetic amine (NTA) functionalized nanoparticles obtained by aqueous polymerization-induced self-assembly (PISA) are introduced as immobilization supports for polyhistidine-functionalized (His-tagged) enzymes. A novel initiator for nitroxide-mediated polymerization based on the nitroxide SG1 and carrying a protected NTA moiety was first synthesized. Size-exclusion chromatography (SEC) and electrospray ionization mass

spectrometry (ESI-MS) proved the ability of this initiator to produce well-defined end-functional vinyl polymers. Subsequently, oligo(ethylene glycol) methacrylate-based macroinitiators were synthesized and chain-extended to form amphiphilic block copolymer nanoparticles, either by nanoprecipitation or by PISA. The latter method yielded spherical nanoparticles with a higher definition, as demonstrated by dynamic light scattering (DLS). Deprotection of the NTA moiety and complexation with nickel ions were assessed by DLS and inductively coupled plasma optical emission spectroscopy/mass spectrometry (ICP-OES/MS). Finally, immobilization of His-tagged horseradish peroxidase and ester hydrolase were successfully carried out, leading to catalytically active nanobiocatalysts, as shown by UV-Vis measurements.

KEYWORDS His tag, protein immobilization, nanobiocatalyst, polymerization-induced self-assembly, nitroxide-mediated polymerization

INTRODUCTION

The immobilization of enzymes is a widely employed method to increase their stability, particularly towards various solute, pH, ionic strength, or temperature conditions, as well as their recyclability.[1-3] The majority of immobilization studies – as well as protein-polymer conjugates – rely on coupling through surface-exposed amino acid residues, which often is non-site specific. However, one of the most important aspects of immobilization is the precise orientation of the biomolecule to reach maximum efficiency.[4,5] Unwanted and non-specific interactions like adsorption or deposition of the protein with the solid support can drastically change the protein structure and the conformation of the active site, which may in turn result in decreased activity. Protein engineering provides a means to control the actual site of attachment at the surface of the

protein, as well as provide additional stabilization.[6] For instance, the expansion of the genetic code by introduction of non-canonical amino acids through point mutations as well as precise posttranslational point modification have emerged.[7-9] In the area of biotechnology, the encoding of protein tags is very popular and well-established.[10-13] These tags are often based on polypeptidic chains and are readily introduced by recombinant DNA methods, typically at one terminus of the chosen biomolecule, offering a greater selectivity while maintaining the protein activity. One of the most well-known examples for protein tags is the so-called polyhistidine tag, commonly termed after the trademark name His-tag.[14-19] This aminoacid sequence consists of six histidine residues. It is practical as its small size usually does not perturb the folding and the activity of the tagged protein, as opposed to larger tags such as SNAP or Halo tags (19.4 and 33 kDa, respectively).[16,20] Through micromolar affinity with metal ions such as Ni^{2+} or Co^{2+} ions, the His-tag can bind to a chelator through a chelate complex. Nitrilotriacetic acid (NTA) is a common chelator because of its three carboxylic acids able to complex Ni^{2+} and form a sandwich complex with the polyhistidine tag. This combination of His-tagged fusion protein and NTA on a solid support is a ubiquitous method for protein isolation and purification, particularly as the complexation can be reversed by the addition of excess imidazole which will compete with the His-tag. Immobilization supports are typically flat surfaces and more often microparticles. However, for biotechnological purposes, it is interesting to go further down the length scale.[4,21] Nanoparticles would indeed provide a significantly larger specific surface area, hence higher concentrations of biocatalysts, while still maintaining the features of a heterogeneous catalyst. The general aim of the current study is indeed to report the synthesis of nanoparticles with the ability to specifically immobilize His-tagged enzymes and yield biocatalytic nanoobjects. This

aim encompasses two aspects: (i) prevention of non-specific protein adsorption and (ii) incorporation of NTA moieties.

We have opted for amphiphilic block copolymers as they provide a facile access to nanoparticles with a wide range of properties. Particularly, by adequate macromolecular design, it is possible to control the surface chemistry of the amphiphilic block copolymer nanoobjects. Here, we have chosen comb-shaped poly(ethylene glycol) derivatives that can be obtained by reversible-deactivation radical polymerization (RDRP). RDRP simultaneously offers straightforward reaction setup and control over polymer chain ends. This was exploited to introduce the NTA moiety at the α chain end of a water-soluble polymer. Chain extension with a hydrophobic segment then led to amphiphilic block copolymers presenting the NTA moiety at their water-soluble end (Scheme 1).

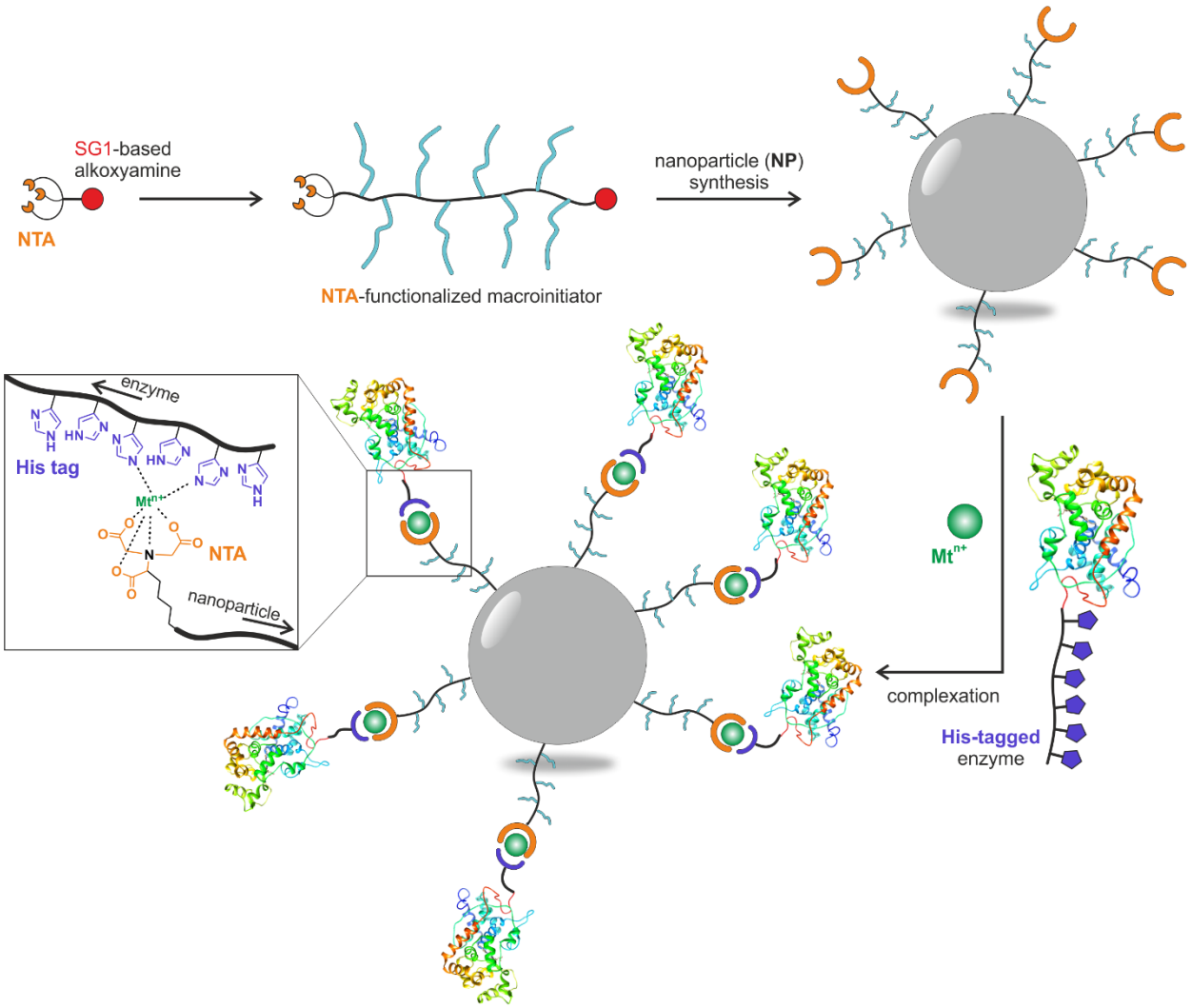

Scheme 1. Designed pathway for obtaining NTA-functionalized polymeric nanoparticles with His-tagged enzymes immobilized on their surfaces.

For the formation of amphiphilic block copolymer nanoparticles, several methods are available.[22,23] The so-called co-solvent method, a form of nanoprecipitation, is often employed and relies on the dissolution of a purified amphiphilic block copolymer in a non-selective solvent (*e.g.*, DMF, THF) followed by the addition of a solvent selective for one of the blocks (usually, water). An alternative method has recently emerged and relies on a reduced number of synthetic steps: in polymerization-induced self-assembly (PISA), with a process based either on emulsion

or dispersion polymerization and starting from a molecularly dissolved macromolecular reagent, the nanoparticles are formed as the solvophobic block of the block copolymer grows. This method allows to produce amphiphilic block copolymers from a soluble hydrophilic homopolymer precursor which is chain-extended using a second monomer in a suitable solvent (*e.g.*, water or lower alcohols). While the second hydrophobic block grows it becomes gradually insoluble, which drives the *in-situ* self-assembly to form AB block copolymer nano-objects. Depending on the solid concentration in the polymerization and the degrees of polymerization (DPs) of the two blocks, spheres or higher order morphologies like worms and vesicles can be obtained.[24] In principle, any living polymerization technique can be used to conduct PISA experiments. While most of the current literature focus on reversible addition-fragmentation chain transfer (RAFT) polymerization, the first reports of genuine PISA were based on nitroxide-mediated polymerization (NMP).[25-29] The field of PISA is rapidly expanding: while most initial studies were dedicated to mechanistic investigations on molar mass control and, most markedly, on morphological control, a recent trend towards the synthesis of functional nanoobjects by PISA seems to emerge.[30,31]

The practical aim of this work was therefore to synthetize a new NMP initiator possessing a His-tag binding motif (NTA) allowing us to produce His-tagged binding nanoparticles. Comb-type, water-soluble macroalkoxyamines based on (oligoethylene glycol) methyl ether methacrylate (POEGMA) were chosen in order to prevent non-specific protein adsorption and to form sterically stabilized nanoparticles. POEGMA is commonly used as a methacrylate alternative to poly(ethylene glycol) (PEG) showing similar antifouling and biocompatibility properties.[32] Nanoparticle synthesis was then investigated by both the co-solvent method and PISA. The

nanoparticles were finally employed for the immobilization of His-tagged horseradish peroxidase and esterase, which yielded catalytically active dispersions.

EXPERIMENTAL PART

Materials. Butyl methacrylate (BzMA; Merck), *tert*-butyl acrylate (tBA; 98%, Sigma-Aldrich), styrene (S; 99.5%, Acros), and oligo(ethylene glycol) methacrylate M_n = 300 ($OEGMA_{300}$; Sigma-Aldrich) were eluted through a basic alumina column (Roth) to remove the inhibitor. Acrylonitrile (AN; 99+%, Acros), *N*-Hydroxysuccinimide (NHS; 98+%, Acros), oligo(ethylene glycol) methacrylate M_n = 950 ($OEGMA_{950}$; Sigma-Aldrich), nickel(II)sulfate hexahydrate (99%, Acros), ethanol (Fischer), and xylene (Roth) were used as received. *N*-(2-methyl-2-propyl)-*N*-(1-diethylphosphono-2,2-dimethylpropyl)-*N*-oxyl) (SG1; 85%),[33] *N*-(2-methyl-2-propyl)-*N*-(1-diethylphosphono-2,2-dimethylpropyl)-*O*-(2-carboxyprop-2-yl) hydroxylamine (MAMA-SG1; 99%),[34] 2-methyl-2-[*N*-*tert*-butyl-*N*-(1-diethoxyphosphoryl-2,2-dimethylpropyl)aminoxy]-*N*-propionyloxysuccinimde (NHS-MAMA-SG1),[35] 2-methyl-2-[*N*-*tert*-butyl-*N*-(1-diethoxyphosphoryl-2,2-dimethylpropyl)aminoxy]-*N*-hydroxyethyl propionamide (HO-MAMA-SG1),[35] and *N*ˇ,*N*ˇ-bis(*tert*-butoxycarbonylmethyl)lysine *tert*-butylester (pNTA-amine, **1**)[36] were obtained following literature procedures.

Characterization Methods.

Nuclear magnetic resonance spectrometry (NMR). ^1H measurements were performed on a Bruker AM 500 spectrometer at 500 MHz. The analytes were dissolved in $CDCl_3$ and the residual solvent peaks were employed for shift correction.

Size exclusion chromatography (SEC). *N*,*N*-dimethylacetamide (DMAc) was used to elute samples with a concentration of 2 g L^{-1} on a Polymer Laboratories PL-GPC 50 Plus Integrated system comprising an autosampler, a PLgel 2,5 μm bead-size guard column (50 × 7.5 mm) followed by three PLgel 5 μm MixedC columns (300 × 7.5 mm), and a flow rate of 1 mL min^{-1}. The SEC system was calibrated against linear poly(methyl methacrylate) standards with molar masses ranging from 700 to 2 × 10^6 Da. The samples were filtered through polytetrafluorethylene (PTFE) membranes with a pore size of 0.2 μm prior to injection.

Electrospray ionization mass spectrometry (ESI-MS). Spectra were recorded on an LXQ mass spectrometer (ThermoFisher Scientific) equipped with an atmospheric pressure ionization source operating in the nebulizer assisted electrospray mode. The instrument was calibrated in the m/z range 195−1822 using a standard mixture containing caffeine, Met-Arg-Phe-Ala acetate (MRFA), and a mixture of fluorinated phosphazenes (Ultramark 1621) (all from Aldrich). A constant spray voltage of 4.5 kV was used. Nitrogen at a dimensionless sweep gas flow rate of 2 (approximately 3 L min^{-1}) and a dimensionless sheath gas flow rate of 5 (approximately 0.5 L min^{-1}) was applied. The capillary voltage, the tube lens offset voltage, and the capillary temperatures were set to 34 V, 90 V, and 275 °C, respectively. The samples were dissolved at a concentration of 0.1 mg mL^{-1} in a mixture of THF and MeOH (3:2) containing sodium trifluoroacetic acid (0.14 μg L^{-1}).

Dynamic light scattering (DLS). DLS measurements were performed on a Zetasizer Nano ZS (Malvern). Nanoparticles obtained from PISA and co-solvent method were not filtered prior to the measurements. Experiments were performed at 25 °C and 10 readouts were taken in 10 independent measurements for each sample with the attenuator set at 10.

Scanning electron microscopy (SEM). Before SEM measurements, all samples were coated with an approximately 5 nm thick gold-platinum film (Bal-Tec/MED020 Coating System, Macclesfield, United Kingdom). Prepared samples were imaged via scanning electron microscope (FEI Philips XL30 FEG-ESEM, Philips, Amsterdam, Netherlands) equipped with an SE detector under high vacuum conditions in SEM mode using an acceleration voltage of 10-20 keV.

Inductively coupled plasma optical emission spectrometry/*mass spectrometry (ICP-OES/MS).* Nickel concentration was determined by optical emission spectrometry (ICP-OES, OPTIMA 4300 DV from PerkinElmer) and mass spectroscopy (ICP-MS, 7500ce from Agilent). 400 µL of each sample (accuracy better than ± 0.8%) was dissolved in 2 mL hydrochloric acid and 8 mL nitric acid at 499 K for 5 min in a microwave (Speedwave Xpert, Berghof). The analysis of Ni content was accomplished with four different calibration solutions and an internal standard (Sc). The range of the calibration solutions did not exceed a decade. Three wavelengths (ICP-OES) and three masses (ICP-MS, 58, 60, 62) of the element were used for calculation.

Experimental Procedures.

Synthesis of pNTA-MAMA-SG1

In a dried Schlenk flask pNTA amine **1** (357.2 mg, 0.80 mmol) was dissolved in dry DCM (5 mL) and deoxygenated by nitrogen bubbling for 20 min at 0 °C. In a second flask NHS-MAMA-SG1 (384.2 mg, 0.80 mmol) was dissolved in dry DCM (10 mL) and deoxygenated by nitrogen bubbling for 20 min at 0 °C. The latter solution was then introduced to the pNTA amine solution

and the resulting mixture was stirred for 2 h at 0 °C. Subsequently, the organic phase was washed three times with H_2O (15 mL), dried over Na_2SO_4, and concentrated under reduced pressure at room temperature. The crude product was purified by silica gel column chromatography using cyclohexane/ethyl acetate (1:1 v/v) to yield pNTA-MAMA-SG1 **2** (356.9 mg, 56%) as a colorless oil. ^{1}H NMR (500 MHz, $CDCl_3$, ●): 7.99 (s, 1H), 4.21–4.06 (m, 4H), 3.46 (q, 4H), 3.33 (s, 1H), 3.24 (m, 1H), 3.01 (brs, 1H), 1.65 (s, 5H), 1.54 (s, 5H), 1.43 (s, 9H), 1.42 (s, 18H), 1.33–1.29 (m, 8H), 1.18 (s, 9H), 1.08 (s, 9H) ppm. MS (ESI, m/z): [M+Na^+] calc.: 816.5110, found: 816.5115.

Solution polymerizations

pNTA-functionalized poly(*t*-butyl acrylate) (pNTA-PtBA)

pNTA-MAMA-SG1 **2** (40.9 mg, 0.05 mmol) and SG1 (1.4 mg, 0.005 mmol) were dissolved in tBA (2.4 mL, 2.27 mmol). This mixture was deoxygenated by five freeze-pump-thaw cycles and subsequently heated to 115 °C for 20 min. After cooling to room temperature, the crude product (22%, 1300 g mol^{-1}) was precipitated in methanol, filtered, and dried under vacuum. This product was further analyzed by direct injection in ESI-MS (see main text). The polymerization was performed anew on a larger scale for 1 h with the same monomer-to-initiator ratio of 45 to analyze the resulting polymer by SEC.

pNTA-functionalizated $POEGMA_{300}$ (**macro1**)

In a typical $OEGMA_{300}$ nitroxide-mediated polymerization, $OEGMA_{300}$ (1.65 mL, 5.67 mmol), styrene (0.04 mL, 0.55), functionalized alkoxyamine initiator **2** (79.1 mg, 0.1 mmol), and SG1 (2.9 mg, 0.08 mmol) were dissolved in xylene (6 mL). The mixture was deoxygenated by six

free-pump-thaw cycles and then heated to 95 °C. Samples were periodically withdrawn to determine monomer conversion using ^{1}H NMR spectroscopy. The polymerization was later performed on a larger scale to produce a sufficient amount of macroinitiator for further experiments. According to the preliminary kinetic study, the reaction was carried out for 18 h and the final product was precipitated in cold pentane, filtered, and dried under vacuum. Characteristics of **macro1** are collated in Table 1.

pNTA-functionalized POEGMA$_{950}$ (**macro2**)

In a typical OEGMA$_{950}$ polymerization, OEGMA$_{950}$ (2.4 g, 2.52 mmol), styrene (0.03 mL, 0.252 mmol), functionalized alkoxyamine initiator **2** (100 mg, 0.12 mmol), and SG1 (0.37 mL, 0.012 mmol) stock solution (10 mg/mL in EtOH) were dissolved in ethanol (9.2 mL) and deoxygenated by nitrogen bubbling for 35 min at room temperature. The mixture was then heated to 79 °C. Samples were periodically withdrawn to follow monomer conversion using ^{1}H NMR spectroscopy. The polymerization was later performed on a larger scale to produce sufficient amounts of macroinitiator for further experiments. According to the preliminary kinetic study, the reaction was carried out for 6 h and the final product was precipitated in diethyl ether, filtered, and dried under vacuum. Characteristics of **macro2** are collated in Table 1.

HO-functionalized POEGMA macroinitiator (**macro3**)

The same recipes as for the pNTA-functionalized macroinitiators above was applied, at the exception that pNTA-MAMA-SG1 was replaced by HO-MAMA-SG1. Characteristics of **macro3** and **macro4** are collated in Table 1.

Table 1. Main characteristics of the macroalkoxyamines utilized as initiators in bulk or emulsion polymerization.

	Structure	target M_n[a]	X_{NMR}[b]	$M_{n,SEC}$[c]	$Đ$[c]
		g mol^{-1}	*%*	*g mol^{-1}*	
macro1	pNTA-P(OEGMA$_{300}$-*co*-S)	17 400	67.3	14 100	1.47
macro2	pNTA-P(OEGMA$_{950}$-*co*-S)	30 700	52.5	21 400	1.24
macro3	HO-P(OEGMA$_{300}$-*co*-S)	7 500	95.1	6 700	1.54
macro4	HO-P(OEGMA$_{950}$-*co*-S)	30 700	13.0	12 500	1.15

[a]*at full conversion.* [b]OEGMA conversion determined by ^{1}H NMR spectroscopy. [c]Experimental M_n obtained by SEC in DMAc using PMMA calibration.

pNTA- and HO-functionalized POEGMA$_{300}$-b-PS amphiphilic block copolymers

In a typical chain extension in homogeneous medium, styrene (0.2 mL, 1.58 mmol) was polymerized in bulk at 120 °C for 1 h, using either **macro1** or **macro3** (49.6 mg, 0.0027 mmol) as macroinitiator. In each case, the crude product was precipitated in cold methanol, filtered, and dried under vacuum to yield either pNTA-(POEGMA$_{300}$-*co*-S)-*b*-PS **pNTA-BCP** (M_n = 98400 g mol^{-1}, $Đ$ = 1.70) and non-functionalized amphiphilic block copolymer HO-(POEGMA$_{300}$-*co*-S)-*b*-PS **HO-BCP** (M_n = 76600 g mol^{-1}, $Đ$ = 1.40).

*Synthesis of NTA-functionalized nanoparticles by the co-solvent method (**NP1**)*

2.0 mg of the functionalized amphiphilic block copolymer NTA-POEGMA$_{300}$-*b*-PS (M_n = 98400 g mol^{-1}, $Đ$ = 1.70) and 13.8 the hydroxyl-functionalized amphiphilic block copolymer HO-POEGMA$_{300}$-*b*-PS (M_n = 76600 g mol^{-1}, Đ = 1.4) were dissolved in filtered THF (2 mL). Through a syringe pump water (18 mL) was added to the organic phase within one hour under

constant stirring. The solution was then dialyzed (MWCO 1 kDa) against water for 24 h to completely remove the THF. (DLS) Z_{av} = 397 nm; σ = 0.149.

Butyl methacrylate polymerization-induced self-assembly (PISA)

In a typical PISA polymerization given amounts of (p)NTA-functionalized macroalkoxyamine **macro2** (20.0 mg, 0.001 mmol) and HO-functionalized macroalkoxyamine **macro4** (40.0 mg, 0.003 mmol) were first dissolved in 1.125 mL water. The monomers BMA (336.7 mL, 2.1 mmol) and styrene (22.0 mL, 0.19 mmol) were added to this solution and the resulting mixture was deoxygenated by nitrogen bubbling for 35 min. The mixture was then heated to 85 °C for 6 h. Characteristics of the obtained polymers and nanoparticles are collated in Table 2.

After PISA experiments the particle solution was dialyzed (MWCO 1 kDa) for 72 h changing the surrounding water 10 times, in order to remove non-polymerized monomers. Dead/unreacted macroinitiator was removed via three washing cycles. Each cycle consisted of three steps: centrifugation (4000 rpm) at 4 °C for 40 min, removing the supernatant containing excess dead macroinitiator, and redispersing the pellet in MilliQ water.

Table 2. Experimental conditions and characteristics of the polymer particles synthesized by polymerization-induced self-assembly of *n*-butyl methacrylate with a low percentage of styrene in water.

entry	**macro2**/**macro4**	[macroinitiator]	target M_n [a]	X_{wt} [b]	M_n ($Đ$) [c]	D_n [d]	PDI [d]
	mol/mol	*mM*	*g mol^{-1}*	*%*	*g mol^{-1}*	*nm*	
NP2	100:0	2.44	84 000	30	35 000 (2.28)	96	0.02
NP3	25:75	2.40	84 000	59	42 600 (1.66)	99	0.02

[a]Molecular weight of resulting block copolymer. [b]Overall monomer conversion determined by gravimetrical analysis. [c]Determined by SEC in DMAc with PMMA standards. [d]Determined by DLS measurements at ambient temperature in water.

Deprotection of pNTA-functionalized nanoparticles

To a nanoparticle dispersion obtained by either PISA or the co-solvent method (0.4 mL), H_3PO_4 (85 wt% in H_2O, 0.15 mL) was added. The mixture was stirred overnight at room temperature and then dialyzed (MWCO 1 kDa) for 24 h, changing the water 4 times in the process.

Nickel complexation with NTA-functionalized nanoparticles

A 1 M $NiSO_4$ solution was prepared in MilliQ water. 200 µL of the nickel solution was added to a small Eppendorf vial containing 1 mL of deprotected NTA-functionalized NP solution. The particle solution was placed on a shaker at ambient temperature for 2 h. Excess Ni^{2+} was removed by three washing cycles. Each cycle consisted of three steps: centrifugation (4000 rpm) at 4 °C for 40 min, removing the supernatant containing excess Ni^{2+}, and redispersing the pellet in MilliQ water. NTA particles complexed with cobalt were prepared as described by Wegner and Spatz.[37]

Production and purification of His-tagged horseradish peroxidase (HRP-His) and His-tagged ester hydrolase (Mes1-His)

Horseradish peroxidase gene (GeneBank code CAA00083.1, from *Armoracia rusticana)* was purchased from Invitrogen and cloned into pET32b+ vector. pET32b+*_hrp* plasmid was transformed into *E. coli* BL21 strain and expressed under β-*D*-1-thiogalactopyranoside (IPTG) induction. The protein was expressed as inclusion bodies, which were separated, purified, and refolded in order to yield pure (> 95%) and active protein. Mes1 ester hydrolase was retrieved from a fosmid clone library created from sediment samples of Messina harbour (Sicily, Italy) (GeneBank code KR107252). The gene encoding Mes1 was cloned into Ek/LIC 46 (Novagen) expression vector using a PCR-based approach, appropriate fosmid DNA sample as template, and *E. coli* BL22 as host.

For further details on cloning, expression, and folding experiments, refer to the SI file.

Enzyme Immobilization

Nanoparticle solutions (50 μL) were mixed with enzyme solutions (200 μL, 1 mg mL^{-1}) in binding buffer (30 mM, 150 mM NaCl, pH 7.4) and stirred for 2 h at RT. Non-bound protein was removed from the polymeric material through 3 centrifugation cycles (14000 x *g*, 10 min) using washing buffer (binding buffer with 50 mM of imidazole). Washed biocatalytic particles were suspended in 75 μL of sodium phosphate buffer (30 mM, pH 7.0) and kept ready for activity assays.

Biocatalytic Assays

Activity measurements were performed using a Biotek Epoch 2 spectrophotometer at 25 °C in 96-well plates. Biocatalytic activity was assayed in triplicate by mixing the enzyme modified nanoparticle suspensions (10 μL) with the adequate substrate (190 μL). Peroxidase activity was evaluated in sodium citrate buffer (50 mM, pH 5.1) with H_2O_2 (2.9 mM) and ABTS (0.27 mM) and ester hydrolase activity in Tris-HCl buffer (50 mM, pH 7.0) with *p*-nitrophenylbutyrate (pNPC4, 0.8 mM). The absorptions arising from oxidized ABTS and the release of *p*-nitrophenol were recorded at 416 and 405 nm, respectively. Initial transformation rates and extinction coefficient values of 36000 $M^{-1}cm^{-1}$ for ABTS and 13400 $M^{-1}cm^{-1}$ for *p*-nitrophenol were used for the calculation of the specific activity.

RESULTS AND DISCUSSION

Synthesis of the NTA-Functionalized NMP Initiator

The first synthetic route we considered to obtain a new NTA-functionalized NMP initiator was a simple coupling between the activated NHS ester of MAMA-SG1 (NHS-MAMA-SG1) and the commercially available NTA amine. However, no common solvent could be found for the two compounds to perform the reaction: Because of its three carboxylic acid groups, NTA could only be solubilized in water, while NHS-MAMA-SG1 would only dissolve in organic solvents. Therefore, an alternative route was used in which the carboxylic acid groups were protected before coupling NTA amine to NHS-MAMA-SG1. The synthesis of the *t*-butyl protected NTA amine **1** consisted of two steps (Scheme 2).[36] After coupling **1** with NHS-MAMA-SG1 and chromatographic purification, the pNTA-functionalized NMP initiator **2** was obtained as a

colorless oil. It was decided to directly employ the protected initiator for polymerization and to hydrolyze the *t*-butyl esters at a later point, *e.g.*, after synthesis of pNTA-functionalized macroinitiator or after nanoparticle formation. There are two reasons for this: (i) the protected form is easier to handle in terms of solubility and (ii) conditions required for the hydrolysis of the *t*-butyl esters may affect the terminal SG1 structure and hamper further chain growth (vide infra).[38,39]

Scheme 2. Complete synthesis of the functional NMP initiator pNTA-MAMA-SG1 **2**.

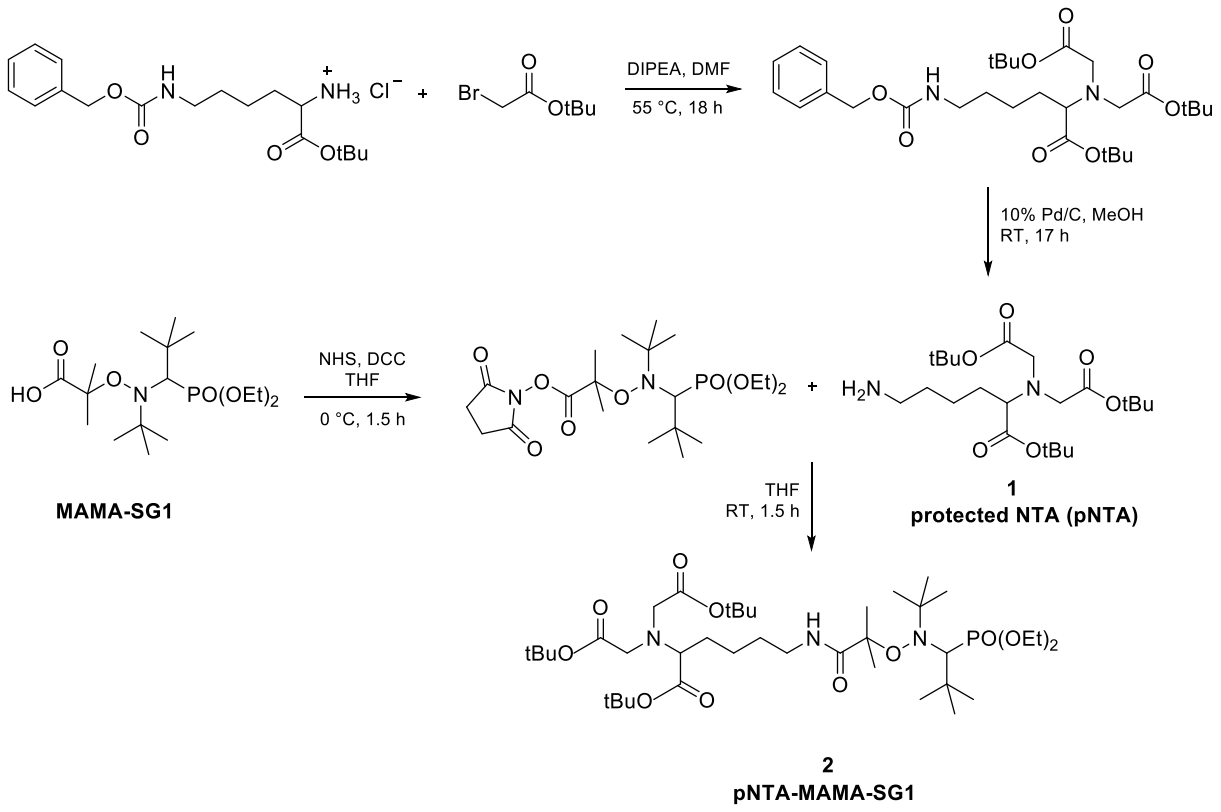

In order to evaluate whether the newly synthesized pNTA-MAMA-SG1 initiator is effective in NMP, *tert*-butyl acrylate bulk polymerization was performed. Two experiments with identical monomer-to-initiator ratios were carried out: one running for 20 min and targeting a low molar mass (M_n < 2000 g mol^{-1}) to allow for electrospray ionization mass spectrometry

characterization and another one with a longer polymerization time (60 min) for clear size-exclusion chromatography analysis.

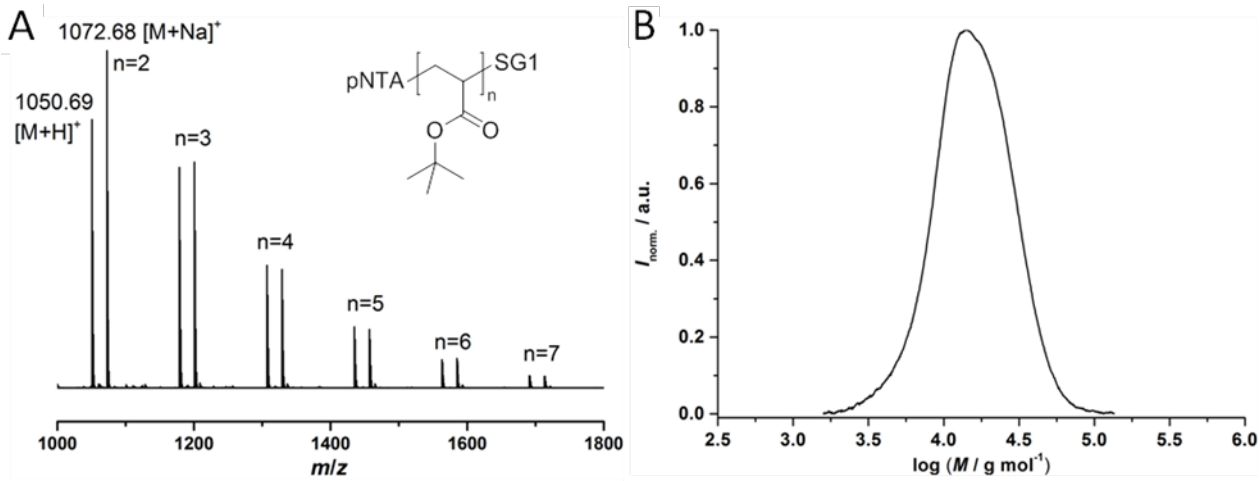

Figure 1. (A) Selected region of the ESI mass spectrum obtained for the short pNTA-PtBA-SG1. (B) SEC traces of pNTA-poly(tBA)-SG1 via NMP. $M_{n,SEC}$ = 13000 g mol^{-1} and $Đ$ = 1.41.

The distribution displayed in the mass spectrum (Figure 1A) correlates with the expected oligomeric structures. The left-most peak doublet corresponds to a tBA dimer with end groups originating from the pNTA-MAMA-SG1 initiator (MW 793.52 g mol^{-1}), with proton and sodium ionization, respectively. The subsequent peaks appearing with increasing m/z values match with the progressive addition of monomer units. From the tBA polymerization with a larger [tBA]/[pNTA-MAMA-SG1] ratio, SEC analysis of the final polymer reveals a reasonable distribution (Figure 1B). Put together, ESI-MS and SEC data indicate that pNTA-MAMA-SG1 can successfully initiate a nitroxide-mediated polymerization and introduce a protected NTA moiety at the alpha extremity of a polymer chain.

Polymerization of Oligo(Ethylene Glycol) Methacrylates and Chain Extension Experiments

Methacrylates were chosen to produce the hydrophilic stabilizing segments because they usually yield more stable polymers than acrylates and particularly enable a lower polymerization temperature in NMP. Yet their SG1-mediated polymerization requires the addition of a small amount of "controlling" co-monomer with a low polymerization constant k_p and a significantly lower NMP equilibrium constant K for the effective control of the polymerization.[40] Two distinct oligo(ethylene glycol) methacrylates with different side-chain lengths were considered to build the protein-repellent, stabilizing, hydrophilic shell of the nanoparticles. Number-average molar masses are 300 and 950 g mol^{-1} for $OEGMA_{300}$ and $OEGMA_{950}$, respectively. While $OEGMA_{300}$ is easier to handle – particularly with regards to polymer purification – it is not suitable for NMPISA because it exhibits a lower critical solubility temperature in water lower (ca. 64 °C) than typical temperatures required for NMP (> 75 °C).[41] Therefore, $OEGMA_{300}$ was employed for the co-solvent method where particles are formed from purified amphiphilic block copolymers synthesized in homogeneous medium and $OEGMA_{950}$ was polymerized to produce a macroinitiator which could then be used for aqueous NMPISA. For the aforementioned reasons, styrene was introduced as a controlling comonomer and preliminary kinetic runs were performed using the pNTA-functionalized initiator **2**.

Scheme 3. Synthetic route toward NTA-functionalized POEGMA-stabilized nanoparticles.

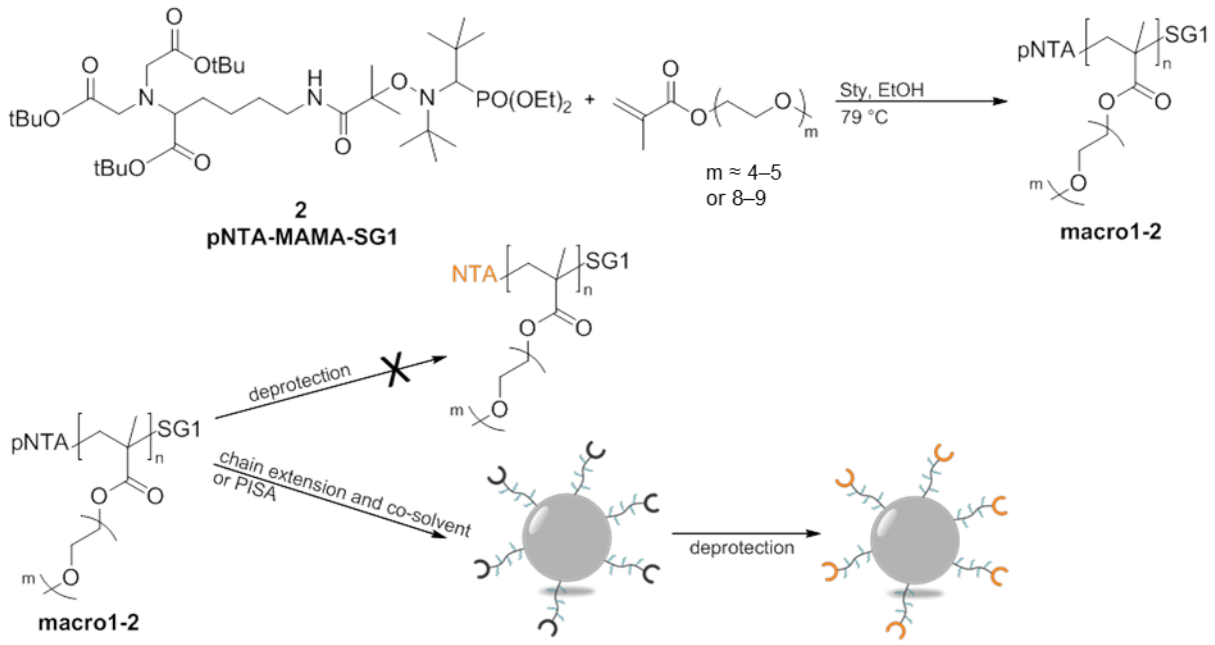

Figure 2 illustrates the evolution of monomer conversion with time, as well as the evolution of the number-average molar mass and dispersity with conversion. The first-order plot of ln[1/(1-conversion)] vs time shows a linear evolution until at least 30% conversion, indicating a constant concentration of propagating radicals in this conversion range. The evolution of M_n determined by size-exclusion chromatography with conversion also follows a linear trend in both cases. Yet, the initiating efficiency does not seem to be quantitative. Compared to unmodified carboxylic acid-based MAMA-SG1, amide-based derivatives are indeed known to possess higher activation energies, which results in non-quantitative initiation.[42] Nevertheless, due to the absence of an adequate SEC calibration and the comb-type character of the POEGMA polymers, definitive conclusions are difficult to draw. Nevertheless, molar masses increasing with conversion (Figure 3), it is possible to choose a desired apparent molar mass.

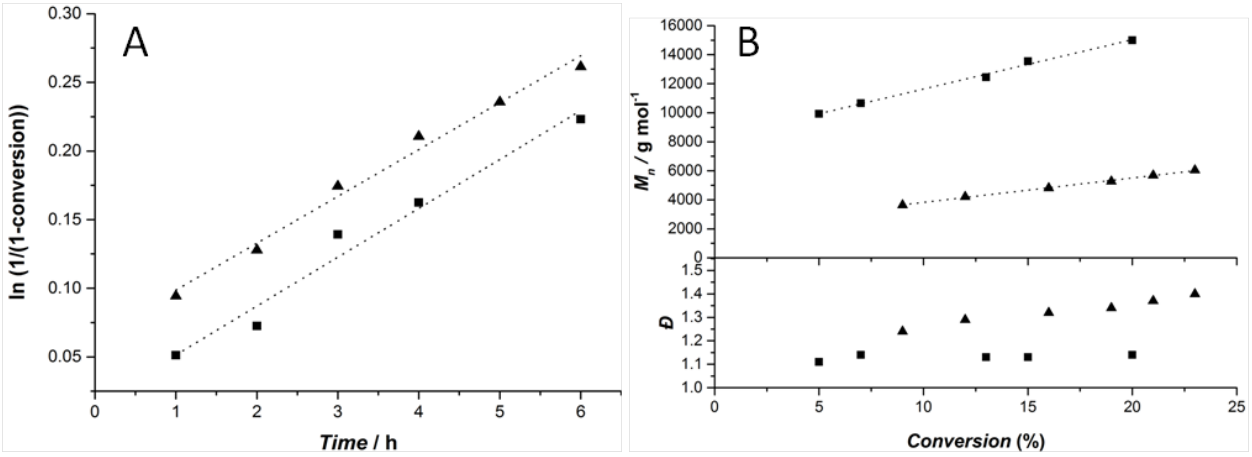

Figure 2. (A) ln[1/(1–*conversion*)] *vs* time and (B) M_n and $Đ$ *vs* conversion plots for the polymerization of $OEGMA_{300}$ (▲) and $OEGMA_{950}$ (■) initiated by pNTA-MAMA-SG1 in the presence of styrene ([OEGMA]/[styrene] = 10). For exact conditions, see the experimental section.

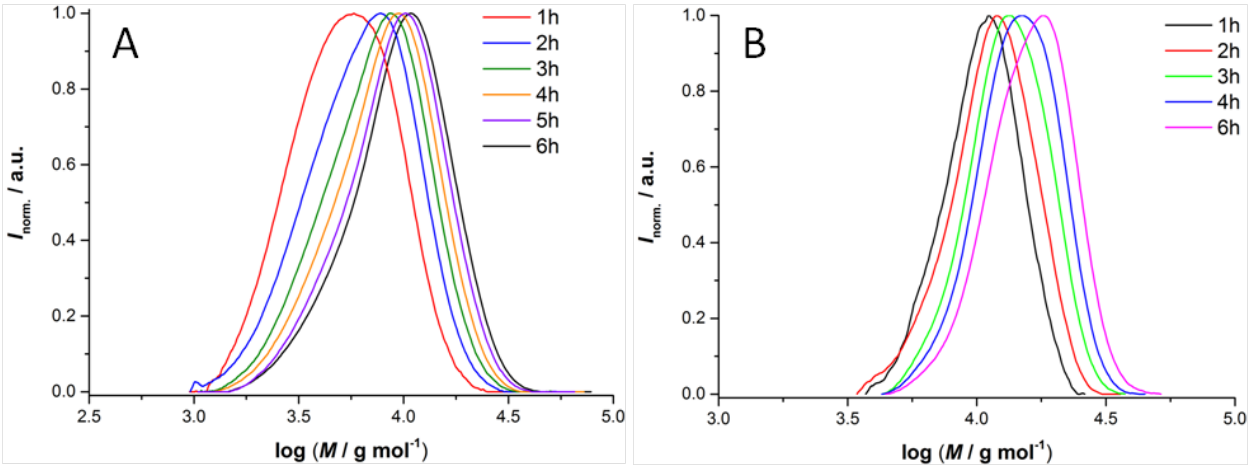

Figure 3. Evolution of the size-exclusion chromatograms during the pNTA-MAMA-SG1-initiated polymerization of (A) $OEGMA_{300}$ in xylene at 95 °C ([OEGMA]/[pNTA-MAMA-SG1] = 57, [OEGMA]/[styrene] = 10, [SG1]/[pNTA-MAMA-SG1] = 0.1) and (B) $OEGMA_{950}$ in ethanol at 79 °C ([OEGMA]/[pNTA-MAMA-SG1] = 32, [OEGMA]/[styrene] = 10, [SG1]/[pNTA-MAMA-SG1] = 0.1).

In order to transform the α end group of the water-soluble macroinitiators into the metal-binding form, the pNTA-functionalized macroinitiator must be deprotected through hydrolysis of the *t*-butyl esters. Trifluoroacetic acid is commonly used for this purpose. Yet it was reported that TFA leads to the cleavage of the *N*-*t*-butyl substituent on the SG1 motif, which in turn deactivates the alkoxyamine thermal lability and hampers re-initiation.[38] We therefore decided to employ a milder deprotection agent, *i.e.*, aqueous phosphoric acid (85 wt% in H_2O). Figure 4 shows a selected region of the ^{1}H NMR spectra of the functionalized macroinitiator before and after deprotection and evidences the effective hydrolysis through the disappearance of the characteristic *t*-butyl protons signal.

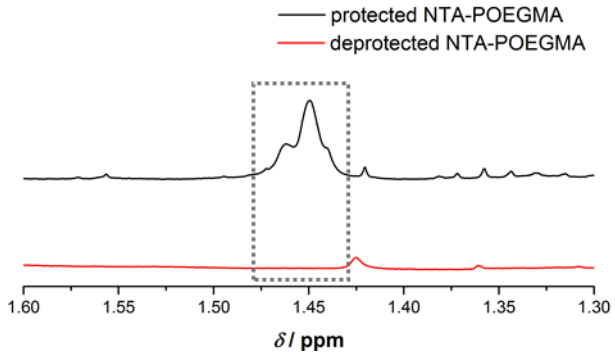

Figure 4. Selected region of the ^{1}H NMR spectra of protected (black) and deprotected (red) macroinitiator. *t*-Butyl peaks at 1.45 ppm (frame) disappear after treatment with phosphoric acid (85 wt% in H_2O) for 24 h and subsequent dialysis.

Synthesis of NTA-Functionalized Core-Shell Nanoparticles

The first route to synthesize NTA-functionalized nanoparticles was the co-solvent method. A mixture of the pNTA- and the HO-functionalized $POEGMA_{300}$-*b*-PS (1:9 mol/mol) was dissolved in THF before water was slowly added to induce self-assembly and form nanoparticles **NP1**. After dialysis to remove THF, the nanoparticles were analyzed by dynamic light scattering

(DLS) and scanning electron microscopy (SEM). While DLS measurements suggested a slightly broad yet monomodal distribution of rather large nanoparticles, the SEM image revealed the presence of a variety of morphologies including donuts, rods and spherical nano- to microstructures. Due to this lack of control over the particle morphology, an alternative route (PISA) was investigated.

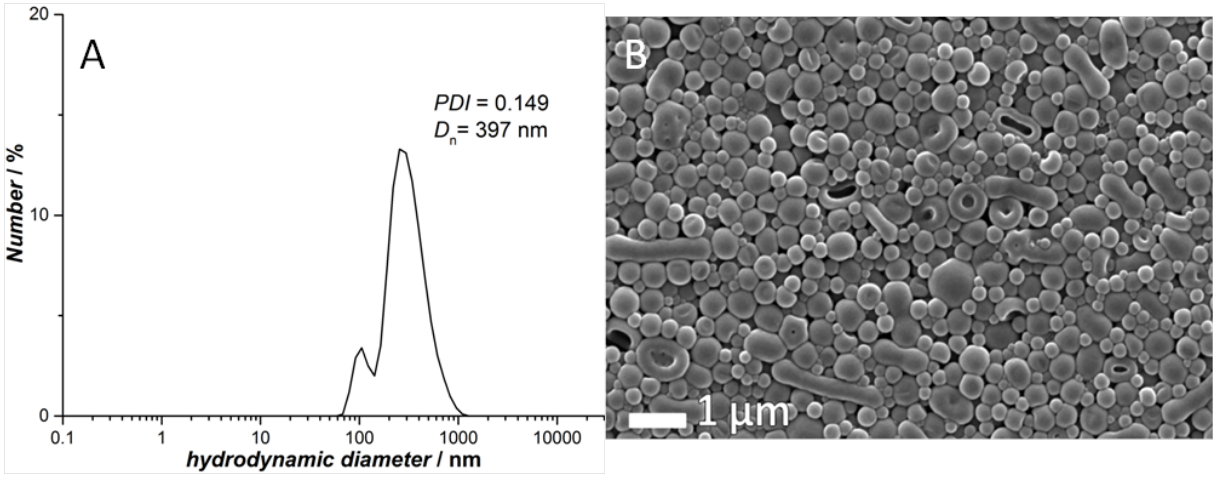

Figure 5. (A) Number-average hydrodynamic diameter distribution of the pNTA-functionalized nanoparticles **NP1** obtained by the co-solvent method and (B) corresponding SEM image.

Polymerization-Induced Self-Assembly

PISA is an elegant alternative for particle formation to the co-solvent method. It possesses the advantages of proceeding through a reduced number of synthetic steps and the possibility to readily access various nanoobject morphologies such as spheres, vesicles, and worms, to name only the most common ones.[43-45] In the present study, nitroxide-mediated PISA (NMPISA) experiments were first conducted in water using methyl methacrylate as a core-forming monomer (with a small amount of styrene) but resulted in low conversions, even after extended reaction times at various temperatures (not shown). Butyl methacrylate (BMA) is a monomer

which has extensively been used in RAFTPISA, as well as in one report in NMPISA using styrene as a co-monomer. A typical experiment was carried out using the hydrophilic $OEGMA_{950}$-based macroinitiators **macro2** and **macro4** to initiate the dispersion polymerization of BMA in the presence of a small amount of styrene at 85 °C for 6 h. Depending on the [**macro2**]/[**macro4**] ratio, conversions between 30–65% were obtained. Increasing the reaction time beyond 6 h did not lead to higher conversions. In the first NMPISA experiment, the polymerization was initiated with the sole deprotected NTA-functionalized $POEGMA_{950}$ **macro2** in order to obtain 100% surface functionalization on the NPs. The SEC trace after 6 h is shown in Figure 6.

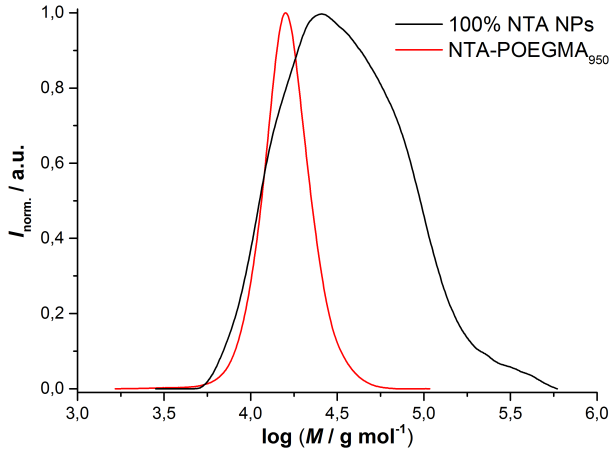

Figure 6. SEC traces of the deprotected functional macroinitiator NTA-$POEGMA_{950}$ (red) and the product of the PISA of BzMA obtained with the deprotected form as sole initiator (black).

Even though the SEC trace shows a shift towards higher molar masses, the distribution is not symmetrical and clearly does not call for a controlled process. Notably, a significant part of the macroinitiator seemed to not react during the polymerization, as indicated by the strong tailing. The reason for this result may lie in the deprotection step of the macroinitiator. As mentioned

previously, aqueous phosphoric acid was employed as milder deprotecting agent for the *t*-butyl esters at the *α* chain end, which could be confirmed by ^{1}H NMR spectroscopy. However, due to low intensity and overlapping of NMR signals, it is difficult to verify whether the *N*-*t*-butyl group being part of the SG1 nitroxide moiety at the ω chain end remains intact during H_3PO_4 treatment. Due to this issue, it was decided to conduct further PISA experiments with **macro2** in its protected form and to proceed to the cleavage of the *t*-butyl esters directly at the surface of the PISA-made nanoparticles.

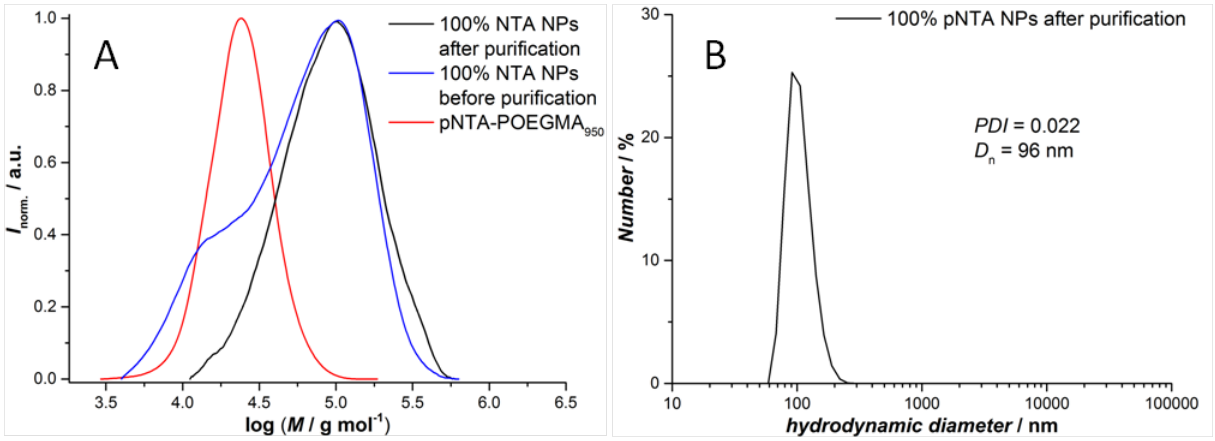

Figure 7. (A) SEC traces of **macro2** (red) and the resulting block copolymer $POEGMA_{950}$-*b*-PBMA obtained by **macro2**-initiated PISA before (blue) and after purification by selective precipitation (black). (B) Corresponding DLS number-average distribution.

The SEC characterization of the PISA-made copolymer is shown in Figure 7A. Again, the chain extension did not proceed ideally. Yet, an improvement was noticeable and further analysis after selective precipitation (to remove unreacted POEGMA chains) proved that a significant fraction of the macroinitiator participated in the reaction, leading to a pNTA-P(OEGMA-*co*-S)-*b*-PBMA amphiphilic block copolymer (see Figure S5). The causes of incomplete initiation are still

unclear. Indeed, during the synthesis of **macro2**, the polymerization seemed rather well controlled (Figure 7). Yet it is also known that for increasing conversion during the NMP of methacrylates by the copolymerization approach a fraction of dead chains constantly accumulates.[46] Furthermore, given the high molar mass of the monomer $OEGMA_{950}$, it is also possible that the number of incorporated styrene units in chains of $M_n < 20000$ g mol^{-1} is too low to guarantee that all chains carry the terminal sequence OEGMA-S-SG1 necessary for adequate reinitiation, as suggested in relevant experiments reported by Bourgeat-Lami, Charleux, and co-workers.[47] Nevertheless, a stable dispersion **NP2** of nanoparticles displaying pNTA moieties at their surface could be obtained with a narrow distribution of hydrodynamic diameters centered (D_n = 96 nm; Figure 7B). NTA-functionalized nanoparticles were obtained after treatment of **NP2** with aqueous phosphoric acid in water and subsequent dialysis and centrifugation steps. The purified SEC trace of the 100% functionalized NPs is shown in Figure 7.

To tune the number of immobilized proteins and therefore modulate the enzymatic activity of the nanoparticles, we prepared a second dispersion (**NP3**) by mixing **macro4** (HO-functionalized $POEGMA_{950}$) with **macro2** for initiation of PISA (3:1 mol/mol), which has the effect of diluting (p)NTA moieties at the surface of the nanoparticles with non-binding hydroxyl moieties. Resulting SEC traces before and after purification are shown in Figure 8A. A shift towards higher molecular weights confirms successful block copolymer formation. However the unpurified product showed a tailing indicating unreacted macroinitiator which was removed via five centrifugation cycles. The resulting supernatants were analyzed and after the last centrifugation cycle the unreacted macroinitiator was removed completely. As **NP2**, **NP3** exhibits a narrow distribution of nanoparticles with an average hydrodynamic diameter of about 97 nm (Figure 8 B). The particles were deprotected and purified afterwards as mentioned above.

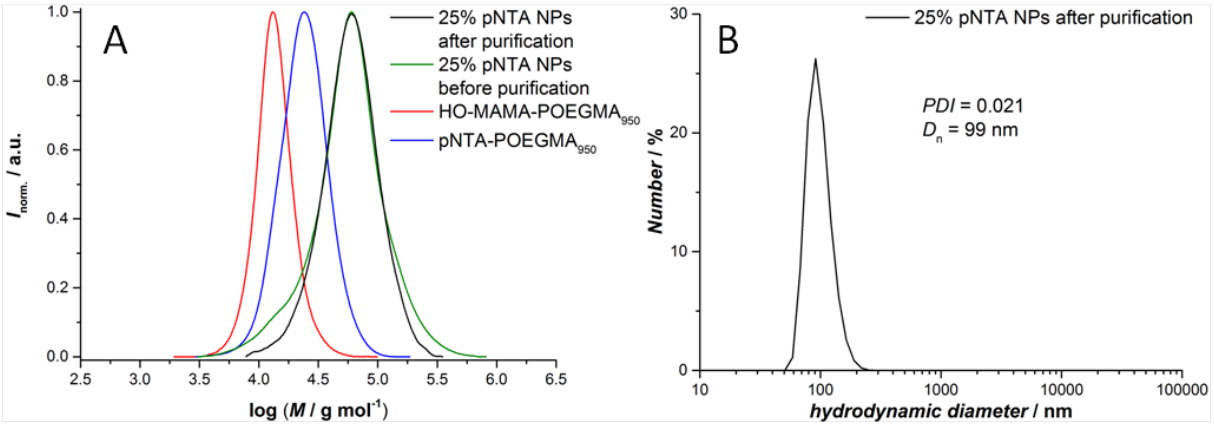

Figure 8. (A) SEC traces of the **macro2** (blue) and **macro4** (red) and the corresponding block copolymer $POEGMA_{950}$-*b*-PBMA obtained by PISA andcontaining the 25 mol% of anchoring pNTA group, before deprotection (**NP3**). (B) Corresponding DLS number-average distribution.

Metal Complexation

The deprotected nanoparticle dispersions **NP2** and **NP3** were then subjected to metal complexation in order to evidence their ability to complex His-tagged proteins. Particularly, Ni^{2+} is commonly employed for this purpose. The DLS data obtained from these NP solutions before and after deprotection and after nickel complexation are shown in Figure 9. In this case, intensity distributions are presented as they allow a better assessment of the successive steps until enzyme immobilization (see further). For number distributions, please refer to the Supporting Information (Figure S6). Before deprotection (red) or after deprotection and nickel complexation (black), both nanoparticle dispersions show a very narrow size distribution and an intensity-average particle size between 110–130 nm after purification and Ni^{2+} complexation, with minor variations.

Inductively coupled plasma mass spectrometry (ICP-MS) was performed to determine the amount of nickel complexed by the particles (see Supporting Information for full calculations).

An average of 8100 and 3200 Ni^{2+} ions per nanoparticle were calculated for **NP2** and **NP3**, respectively (100% and 25% NTA functionalization, respectively). In addition, this would imply that each nickel atom occupies an area of 3.6 and 9.6 nm^2 or, in other terms, is separated from its immediate neighbors by only about 1.1 to 1.7 nm in average, for **NP2** and **NP3**, respectively. Dimensional considerations with respect to protein diameter therefore suggest that in both cases only a fraction of NTA/Ni^{2+} complexes will be able to participate in enzyme immobilization.

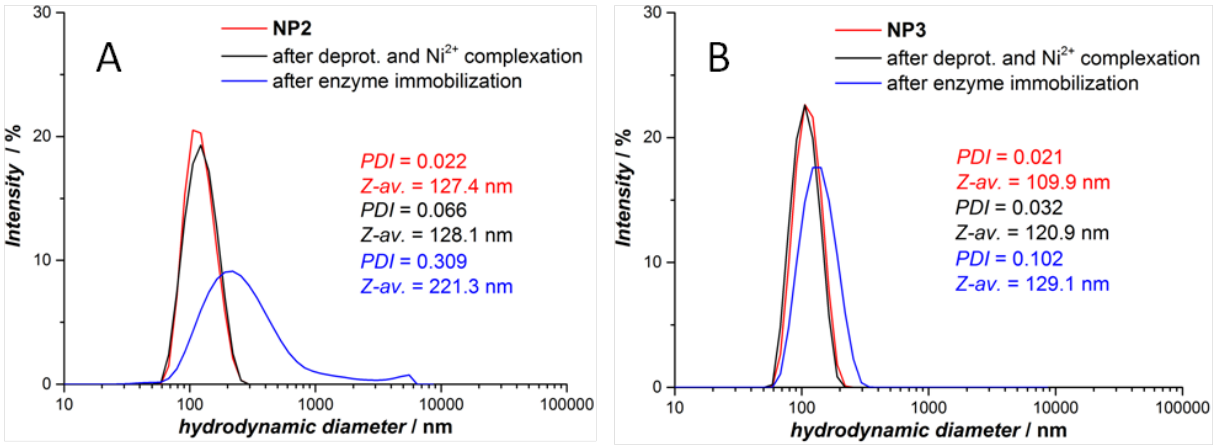

Figure 9. Intensity-average hydrodynamic diameter distributions of the NTA-functionalized NPs obtained by PISA: (A) 100% NTA functionalization and (B) 25% NTA functionalization, before deprotection (red), after deprotection and Ni^{2+} complexation (black), and after double His-tagged HRP immobilization (blue).

Enzyme Immobilization and Activity of the Nanobiocatalysts

Finally, we aimed to demonstrate that these NTA-functionalizated NPs can be used as solid support for His-tagged recombinant proteins. We selected two biocatalysts with different substrate specificity, *i.e.*, horseradish peroxidase (HRP) and ester hydrolase (Mes1). The fusion of a His-tag to the *N*-termini of the primary sequence of both proteins led to HRP-His and Mes1-

His recombinant proteins and enabled us to address the protein tethering to NTA-bearing nanoparticles through metal ion coordination.

NP1 particles were employed for preliminary assessment of the ability to immobilize His-tagged proteins. Nickel and cobalt were selected as metals for NTA coordination and used to produce HRP-His_Ni_NP1, HRP-His_Co(II)_NP1, and HRP-His_Co(III)_NP1 nanohybrids. The latter was obtained after the soft oxidation of HRP-His_Co(II)_NP1 with hydrogen peroxide, as described by Wegner and Spatz.[37] After introduction of HRP-His in dispersions of NP1 previously incubated with either Ni or Co ions, unspecifically bound protein was removed by washing with 50 mM imidazole. Non-deprotected **NP1** particles were used to observe the occurrence of non-specific adsorption between the protein and the particles. As shown in Figure S7 (right, black dots), no activity was detected for non-deprotected **NP1**. This shows that pNTA is unable to bind enzymes, which demonstrates at the same time the protein-repellent character of the POEGMA-based shell. We also observed a higher ABTS oxidation activity for HRP-His_Co(III)_NP1 (0.0068 nmol min^{-1} μL^{-1}) followed by HRP-His_Ni_NP1 (0.0037 nmol min^{-1} μL^{-1}) and HRP-His_Co(II)_NP1 (0.0015 nmol min^{-1} μL^{-1}). However, cobalt-containing particles resulted in aggregates which precipitated (see inset in Figure S7, left), leading to no reproducible results. For this reason, nickel was used as coordination metal for the next experiments.

Next, we enquired whether the PISA-made, better defined NTA/Ni^{2+}-functionalized **NP2** and **NP3** would be able to immobilize His-tagged proteins in the same manner as **NP1**. Gratifyingly, we successfully anchored HRP-His and Mes1-His recombinant proteins to both **NP2** and **NP3** particles (Figure 10) and were able to examine the effect of the diluting, non-functional macroinitiator introduced in **NP3**. The DLS results obtained with HRP-His are also presented in Figure 9 (blue traces). While only a small variation of the diameter is observed for the lower

NTA content (**NP3**, Figure 9B) yet with a slight increase in dispersity, the diameter of the nanoobjects increase significantly with **NP2**, possessing a higher functionality. This can be explained by the bifunctional nature of the HRP employed in the present study. Indeed, it possesses in fact two His tags, one at both the *N*- and the *C*-termini. Therefore, nanoparticle bridging is likely to have occurred. This however must have remained as a marginal event, if one considers the number-average distribution (Figure S6A). In any case, for both **NP2** and **NP3** systems, active nanobiocatalysts were obtained.

For both enzymes, similar results were achieved when we compared the effect of the dilution of NTA groups on the surface of the particles over the k_{cat} kinetic parameter of the immobilized enzymes: the values for **NP2** (2120 ± 100 min^{-1} for HRP-His and 13720 ± 395 min^{-1} for Mes1-His) dropped to 750 ± 10 min^{-1} and 6700 ± 280 min^{-1} (2.8 and 2.0-fold reduction, respectively) when **NP3** was used as solid support (Figure 10). Since the kinetic parameters are independent of enzyme concentration, the fact that the particles **NP2** (with 100% NTA functionalization) perform better cannot be simply explained. Yet, since **NP3** exhibit a lower surface enzyme functionalization, it is possible that in this case the non-functionalized POEGMA stabilizing chains surrounding the enzymes may hinder protein activity, *e.g.*, by influencing substrate diffusion or shielding the active site. Nevertheless, it can be concluded that our NTA-functionalized nanoparticles successfully lead to the formation of efficient nanobiocatalysts, which can be easily recovered by simple centrifugation.

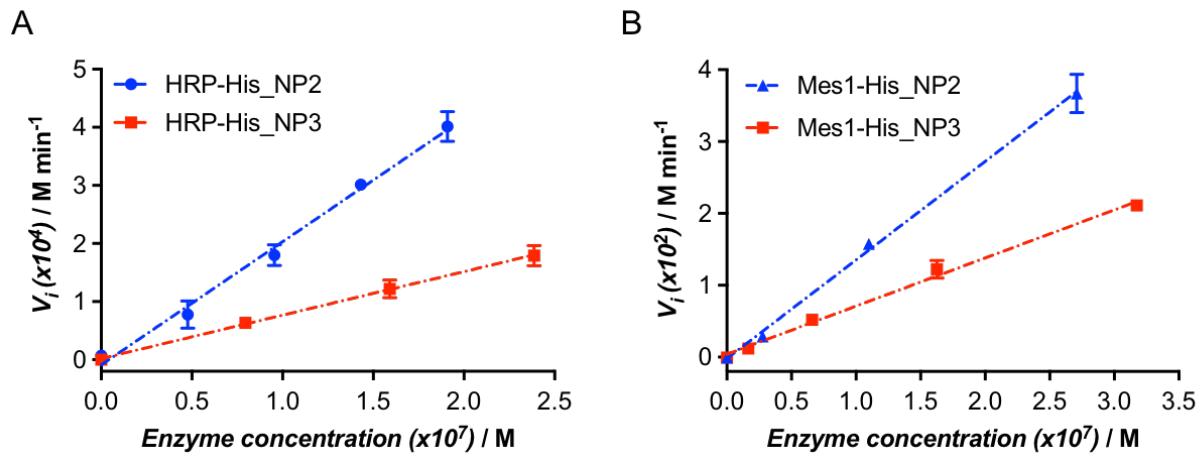

Figure 10. Initial velocity *vs* enzyme concentration plots for (A) HRP-His_NP2 and HRP-His_NP3 and (B) Mes1-His_NP2 and Mes1-His_NP3. The slope of the linear regression represents k_{cat}.

CONCLUSION

In this study, we successfully synthesized a new protected NTA-functionalized SG1-based NMP initiator, which was used to polymerize $POEGMA_{300}$ and $POEGMA_{950}$ macroinitiators. The former was useful to produce amphiphilic block copolymers in solution, which could then be self-assembled by nanoprecipitation, leading to nanoparticles with however a large distribution and various morphologies. The latter, exhibiting full solubility in water at the polymerization temperature, enabled the PISA process to be employed. This permitted the synthesis of nanoparticles with a narrow distribution in the 100 nm range. All nanoparticles, after deprotection of the NTA moiety, were able to induce the specific attachment of His-tagged enzymes such as horseradish peroxidase and esterase. Varying the amount of functional groups through synthetic design allowed for the control of the catalytic activity: the higher the NTA content, the higher the activity. PISA is a very versatile tool giving access to different

morphologies depending on the degree of polymerization. In the current study only spherical nanoparticles were obtained and used for enzyme immobilization. In the future, it would be of interest to extend this work towards the production of nanofibers, which could lead to biocatalytic materials with specific physical properties, *e.g.*, gels. In addition, further protein fusion tags, e.g., SNAP, Halo, or CLIP tags, should be considered in order to lead to multifunctional systems with controlled properties.

ASSOCIATED CONTENT

Supporting Information. Additional synthetic procedures, characterization data, enzymatic assays, as well as calculations for determination of the nickel content.

AUTHOR INFORMATION

Corresponding Author

*E-mail guillaume.delaittre@kit.edu (G.D.).

Present Addresses

†Present Address: Nanomaterials group, CICnanoGUNE, Avenida Tolosa 76, 20018 Donostia-San Sebastián, Spain

ACKNOWLEDGEMENTS

GD would like to thank the German Federal Ministry of Education and Research (BMBF) for current funding in the frame of the Molecular Interaction Engineering program (Biotechnologie 2020+). MF would like to acknowledge funding from the European Union Horizon 2020 research and innovation program [Blue Growth: Unlocking the potential of Seas and Oceans] under grant agreement no. [634486] (project acronym INMARE) and from the Spanish Ministry of Economy, Industry, and Competitiveness (grants PCIN-2014-107 within the ERA NET IB2, and BIO2014-54494-R). AB would like to thank Diputación de Gipuzkoa for current funding in the frame of *Gipuzkoa Fellows* program. We are grateful to Dr Hartmut Gliemann and Tawheed Mohamed (both IFG, KIT) for access to and support on the scanning electron microscope, as well as to Dr Pavel Levkin (ITG, KIT) for providing access to the DLS instrument. ICP-OES/MS measurements were carried out with support of the Karlsruhe Nano Micro Facility (KNMF), a Helmholtz research infrastructure at Karlsruhe Institute of Technology (KIT). The Soft Matter Synthesis laboratory (KIT, Helmholtz BIFTM program) is acknowledged for instrumentation support. Prof. Christopher Barner-Kowollik (ITCP, KIT) is thanked for constant support.

REFERENCES

(1) Bornscheuer, U. T. Angew. Chem. Int. Ed. 2003, 42, 3336.

(2) Hanefeld, U.; Gardossi, L.; Magner, E. Chem. Soc. Rev. 2009, 38, 453.

(3) Rodrigues, R. C.; Ortiz, C.; Berenguer-Murcia, A.; Torres, R.; Fernandez-Lafuente, R. Chem. Soc. Rev. 2013, 42, 6290.

(4) Algar, W. R.; Prasuhn, D. E.; Stewart, M. H.; Jennings, T. L.; Blanco-Canosa, J. B.; Dawson, P. E.; Medintz, I. L. Bioconjugate Chem. 2011, 22, 825.

(5) Liu, Y.; Yu, J. Microchim. Acta 2016, 183, 1.

(6) Hernandez, K.; Fernandez-Lafuente, R. Enzyme Microb. Technol. 2011, 48, 107.

(7) Kim, C. H.; Axup, J. Y.; Schultz, P. G. Curr. Opin. Chem. Biol. 2013, 17, 412.

(8) Deepankumar, K.; Nadarajan, S. P.; Mathew, S.; Lee, S.-G.; Yoo, T. H.; Hong, E. Y.; Kim, B.-G.; Yun, H. ChemCatChem 2015, 7, 417.

(9) Chen, Y.-X.; Triola, G.; Waldmann, H. Acc. Chem. Res. 2011, 44, 762.

(10) Terpe, K. Appl. Microbiol. Biotechnol. 2003, 60, 523.

(11) Kimple, M. E.; Brill, A. L.; Pasker, R. L. In Current Protocols in Protein Science; John Wiley & Sons, Inc.: 2001.

(12) Costa, S.; Almeida, A.; Castro, A.; Domingues, L. Front. Microbiol. 2014, 5, 63.

(13) Lotze, J.; Reinhardt, U.; Seitz, O.; Beck-Sickinger, A. G. Mol. BioSyst. 2016, 12, 1731.

(14) Porath, J.; Carlsson, J.; Olsson, I.; Belfrage, G. Nature 1975, 258, 598.

(15) Gaberc-Porekar, V.; Menart, V. Chem. Eng. Technol. 2005, 28, 1306.

(16) Los, G.; Darzins, A.; Karassina, N.; Zimprich, C.; Learish, R.; McDougall, M.; Encell, L.; Friedman-Ohana, R.; Wood, M.; Vidugiris, G. Cell Notes 2005, 11, 2.

(17) Nehring, R.; Palivan, C. G.; Casse, O.; Tanner, P.; Tüxen, J.; Meier, W. Langmuir 2009, 25, 1122.

(18) Gautrot, J. E.; Huck, W. T. S.; Welch, M.; Ramstedt, M. ACS Appl. Mater. Interfaces 2010, 2, 193.

(19) Xu, F.; Geiger, J. H.; Baker, G. L.; Bruening, M. L. Langmuir 2011, 27, 3106.

(20) Keppler, A.; Gendreizig, S.; Gronemeyer, T.; Pick, H.; Vogel, H.; Johnsson, K. Nat. Biotechnol. 2003, 21, 86.

(21) Ansari, S. A.; Husain, Q. Biotechnol. Adv. 2012, 30, 512.

(22) Peltonen, L.; Koistinen, P.; Karjalainen, M.; Häkkinen, A.; Hirvonen, J. AAPS PharmSciTech 2002, 3, 52.

(23) Govender, T.; Stolnik, S.; Garnett, M. C.; Illum, L.; Davis, S. S. J. Controlled Release 1999, 57, 171.

(24) Karagoz, B.; Esser, L.; Duong, H. T.; Basuki, J. S.; Boyer, C.; Davis, T. P. Polym. Chem. 2014, 5, 350.

(25) Delaittre, G.; Nicolas, J.; Lefay, C.; Save, M.; Charleux, B. Chemical Communications 2005, 614.

(26) Delaittre, G.; Nicolas, J.; Lefay, C.; Save, M.; Charleux, B. Soft Matter 2006, 2, 223.

(27) Delaittre, G.; Save, M.; Charleux, B. Macromolecular Rapid Communications 2007, 28, 1528.

(28) Delaittre, G.; Charleux, B. Macromolecules 2008, 41, 2361.

(29) Delaittre, G.; Dire, C.; Rieger, J.; Putaux, J.-L.; Charleux, B. Chemical Communications 2009, 2887.

(30) Jones, E. R.; Semsarilar, M.; Blanazs, A.; Armes, S. P. Macromolecules 2012, 45, 5091.

(31) He, W.-D.; Sun, X.-L.; Wan, W.-M.; Pan, C.-Y. Macromolecules 2011, 44, 3358.

(32) Xu, F. J.; Li, H. Z.; Li, J.; Teo, Y. H. E.; Zhu, C. X.; Kang, E. T.; Neoh, K. G. Biosens. Bioelectron. 2008, 24, 773.

(33) Hlalele, L.; Klumperman, B. Macromolecules 2011, 44, 6683.

(34) Harrisson, S.; Couvreur, P.; Nicolas, J. Polym. Chem. 2011, 2, 1859.

(35) Vinas, J.; Chagneux, N.; Gigmes, D.; Trimaille, T.; Favier, A.; Bertin, D. Polymer 2008, 49, 3639.

(36) Kadir, M. A.; Park, J. H.; Lee, J.; Lee, C.; Lee, S. H.; Lee, S. G.; Paik, H. j. Macromol. Chem. Phys. 2013, 214, 2027.

(37) Wegner, S. V.; Spatz, J. P. Angew. Chem. Int. Ed. 2013, 52, 7593.

(38) Trimaille, T.; Mabrouk, K.; Monnier, V. r.; Charles, L.; Bertin, D.; Gigmes, D. Macromolecules 2010, 43, 4864.

(39) Barrère, C.; Chendo, C.; NT Phan, T.; Monnier, V.; Trimaille, T.; Humbel, S.; Viel, S.; Gigmes, D.; Charles, L. Chem. Eur. J. 2012, 18, 7916.

(40) Guégain, E.; Guillaneuf, Y.; Nicolas, J. Macromol. Rapid Commun. 2015, 36, 1227.

(41) Lutz, J. F. J. Polym. Sci. A Polym. Chem. 2008, 46, 3459.

(42) Guégain, E.; Delplace, V.; Trimaille, T.; Gigmes, D.; Siri, D.; Marque, S. R.; Guillaneuf, Y.; Nicolas, J. Polym. Chem. 2015, 6, 5693.

(43) Charleux, B.; Delaittre, G.; Rieger, J.; D'Agosto, F. Macromolecules 2012, 45, 6753.

(44) Zehm, D.; Ratcliffe, L. P. D.; Armes, S. P. Macromolecules 2013, 46, 128.

(45) Zhang, X.; Rieger, J.; Charleux, B. Polym. Chem. 2012, 3, 1502.

(46) Lessard, B.; Marić, M. J. Polym. Sci. A Polym. Chem. 2009, 47, 2574.

(47) Qiao, X.; Lansalot, M.; Bourgeat-Lami, E.; Charleux, B. Macromolecules 2013, 46, 4285.